Dalton Transactions

Accepted Manuscript

This is an *Accepted Manuscript*, which has been through the RSC Publishing peer review process and has been accepted for publication.

Accepted Manuscripts are published online shortly after acceptance, which is prior to technical editing, formatting and proof reading. This free service from RSC Publishing allows authors to make their results available to the community, in citable form, before publication of the edited article. This *Accepted Manuscript* will be replaced by the edited and formatted *Advance Article* as soon as this is available.

To cite this manuscript please use its permanent Digital Object Identifier (DOI®), which is identical for all formats of publication.

More information about *Accepted Manuscripts* can be found in the **Information for Authors**.

Please note that technical editing may introduce minor changes to the text and/or graphics contained in the manuscript submitted by the author(s) which may alter content, and that the standard **Terms & Conditions** and the **ethical guidelines** that apply to the journal are still applicable. In no event shall the RSC be held responsible for any errors or omissions in these *Accepted Manuscript* manuscripts or any consequences arising from the use of any information contained in them.

Binuclear ruthenium η^6-arene complexes with tetradentate *N,S*-ligands containing the *ortho*-aminothiophenol motif

Alberto Acosta-Ramirez[a], Edward D. Cross[a], Robert McDonald[b] and Matthias Bierenstiel*[a]

[a] *Cape Breton University, Department of Chemistry, 1250 Grand Lake Road, Sydney, Nova Scotia, B1P 6L2, Canada. Tel: +1 902 5631391; E-mail: Matthias_Bierenstiel@cbu.ca*

[b] *X-Ray Crystallography Laboratory, Department of Chemistry, University of Alberta, Edmonton, Alberta, T6G 2G2, Canada.*

Abstract

A series of cationic binuclear (η^6-cymene-Ru)$_2$ complexes with N_2S_2-ligands were synthesized in 64% to 85% yield by reaction of [Ru(η^6-cymene)Cl$_2$]$_2$ with *bis*-*S,S'*-(*ortho*-aminothiophenol)-xylenes as BF_4^- and PF_6^- salts. The compounds were studied using NMR, HRMS, UV-vis and IR spectroscopy, EA and inductively coupled plasma (ICP) MS. It was determined that the binuclear Ru complexes were *anti* and *syn* diastereomers obtained in 2:1 ratio for *ortho*- and *meta*-xylylene bridged ligands and in a 1:1 ratio for the *para*-xylylene bridged ligand. An anion effect was found for the presence of $NaBF_4$ with the *meta*-xylylene bridged system yielding the targeted binuclear Ru complex and a mononuclear Ru complex. This mononuclear *S,S'*-coordinated η^6-cymene Ru chloride structure lacked amine-metal coordination and was obtained in a 1:3 ratio of *anti*:*syn* diastereomers which were insoluble in CH_2Cl_2 and soluble in DMSO and DMF. X-ray crystallographic analysis was obtained for the N_2S_2 ligand, 1,2-*bis*{(2-aminophenyl)thiomethyl}benzene, showing a C_S symmetry with amine groups facing outwards with a tilt of 28.95° from the *ortho*-aminothiophenol pendant ring. The interatomic sulfur-sulfur distance (S-S') is 4.6405 Å within the crystal structure while accommodating a potential metal bite angle from 1.0 Å to 5.9 Å when allowing rotation of the methylene phenyl bond.

Introduction

Metal-metal synergic interactions in binuclear transition metal complexes have received considerable attention since the discovery by Stanley and co-workers of dirhodium catalysts for hydroformylation reactions.[1, 2] The increased reactivity of metal-metal systems – with or without the presence of intermetallic bonding – is based on concerted mechanisms by activation of a substrate with both metal centres or by sequential activation of two substrates, one at each metal centre.[3-11] Binuclear transition metal complexes can generate mixed-valent species that can be exploited for electronic and magnetic applications. These complexes can be further enhanced with ligands that have non-innocent properties. Weighardt and co-workers reported *ortho*-dithiolene and *ortho*-aminothiolate ligands complexed to Fe as well as iminothione benzosemiquinonate π-radical ligands.[12, 13] Binuclear complexes provide a great diversity for supramolecular chemistry of anion recognition and metalloreceptors due to their geometry and electrochemical properties.[14-18] Typical ligand systems bridging the two metals are bipyridines, terpyridines, polyacetaldehydes, ethynyl and *para*-substituted phenylene.[19-32] Mono- and binuclear Ru polypyridine complexes display electro- and photochemical properties associated with metal-to-ligand charge transfer transitions.[33-38] Binuclear η^3-allyl- and η^6-arene Ru complexes showed a remarkable absorption in the visible region and electrochemical studies revealed interactions between the two metals, allowing for potential application as molecular wires.[39] *N*-heterocyclic carbene (NHC) complexed η^6-arene Ru compounds show two mutually dependent oxidation processes.[40] η^6-Arene Ru half-sandwich complexes with *bis*(bipyridines) are utilized for the visible light induced photocatalytic splitting of CS_2 to elemental sulfur and a carbon-sulfur polymer.[41] Joulie *et al.* reported molecular switches based on Ru complexed to *N,N'* bipyridines.[42]

Hybrid ligands bearing hard *N* and soft *S* donor atoms can be used, as a chelate or bridging unit, to bind either hard/soft metals.[43, 44] Recently, we have reported the synthesis of *ortho*-aminothiophenol based *N,S*-ligands with *ortho*-, *meta*- and *para*-xylene bridges (**1a-c**).[45, 46] These N_2S_2-ligands are targeted systems for small biomimetic metal models for the analysis of redox-active non-blue/type-II copper enzymes such as peptidylglycine α-hydroxylating monooxygenase (PHM), which is one of the two non-coupled copper ion domains of the bifunctional peptidylglycine α-amidating monooxygenase (PAM, EC 1.14.17.3).[47, 48] Hamaker and co-workers reported structures and reactivities of half-sandwich η^6-arene Ru complexes using *N,S*-ligands based on *ortho*-aminothiophenols, *N*-(aryl-methylene)-*ortho*-alkylthioanilines and *ortho*-thiosalicylimines.[49-52] In addition, binuclear Schiff base ruthenium complexes have been used in ring-closing metathesis and ring-opening metathesis polymerizations.[53] We were interested in examining the *N,S*-Ru chelate within binuclear complexes with various Ru-Ru distances using hybrid, tetradentate N_2S_2-ligands. "Herein, we present the results related to the coordination chemistry of N_2S_2-ligands with η^6-arene Ru centres."

Results and discussion

N_2S_2 Ligand

Xylylene bridged *bis* chelate ligands provide an exceptional ligand platform for hinged binuclear metal complexes as the phenylene ring substitution pattern is structurally rigid while the methylene groups allow some flexibility. Recently, we have reported the synthesis of *ortho*-aminothiophenol based *N,S*-ligands with *ortho*-, *meta*- and *para*-xylene bridges and report herein the X-ray crystallographic analysis of the related 1,2-*bis*{(2-aminophenyl)thiomethyl}benzene,

1b,.[45, 46] The compound has C_2 symmetry with a diametrically arrangement of the pendant *ortho*-aminothiophenol rings (Fig. 1 and 2, Table 1 and 2).

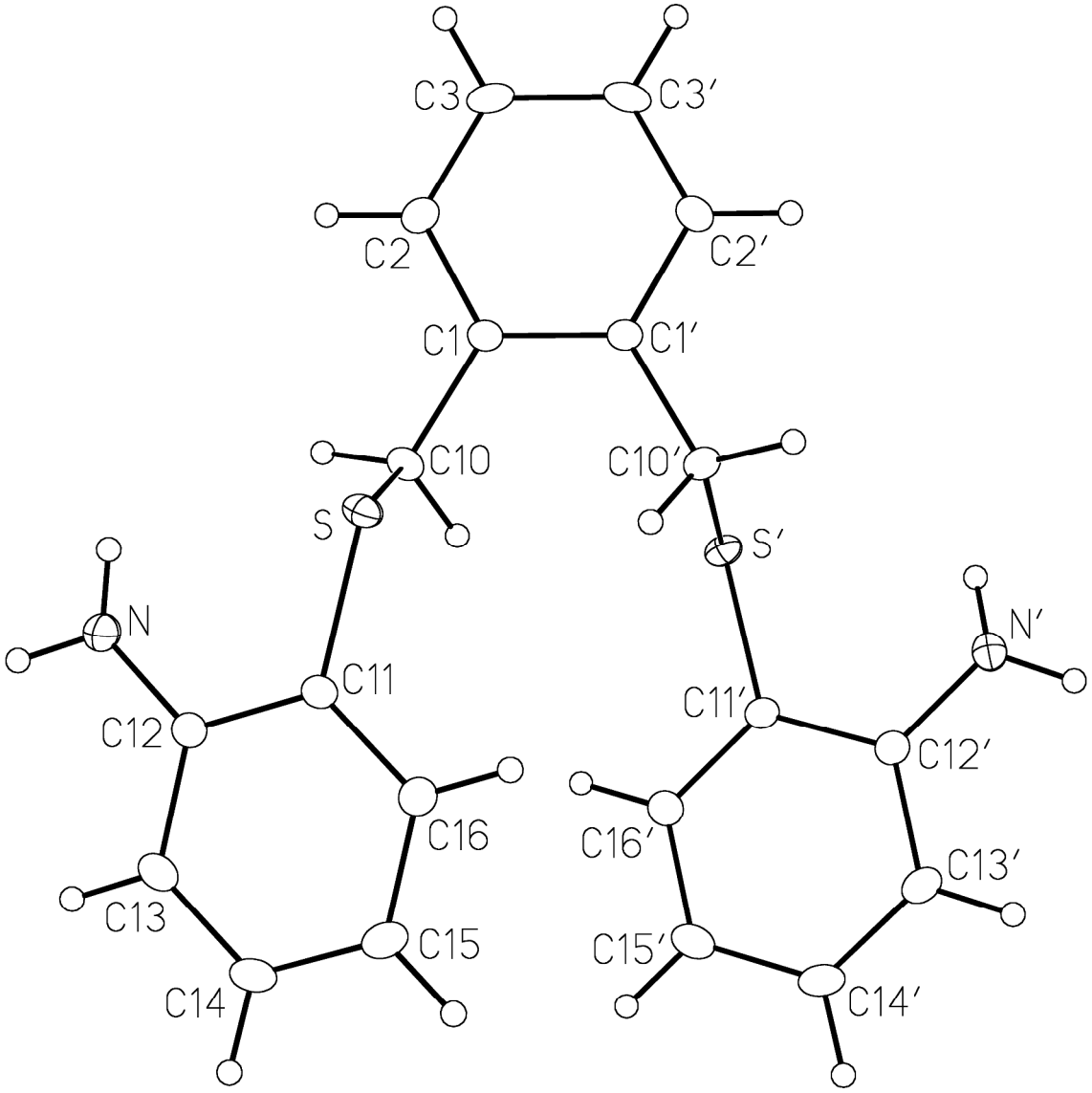

Fig. 1 Perspective view of **1b** showing the atom labelling scheme. Non-hydrogen atoms are represented by Gaussian ellipsoids at the 20% probability level. Hydrogen atoms are shown with arbitrarily small thermal parameters. Primed atoms are related to unprimed ones via the crystallographic twofold axis (0, *y*, 1/4) passing through the midpoints of the C1–C1' and C3–C3' bonds

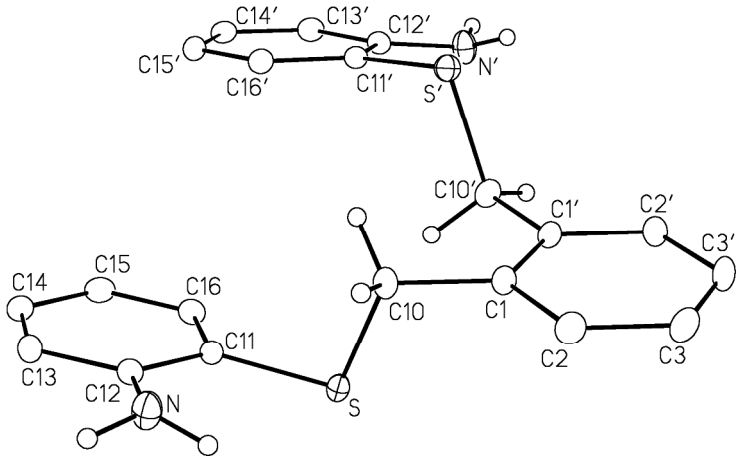

Fig. 2 Alternate view of **1b**. Protons attached to aromatic carbons removed for clarity.

Table 1 Crystallographic Experimental Details

Crystal Data	**1b**
formula	$C_{20}H_{20}N_2S_2$
formula weight	352.50
crystal system	orthorhombic
space group	*Pbcn* (No. 60)
a (Å)	8.4685 (3)
b (Å)	12.1683 (4)
c (Å)	17.2063 (5)
V (Å^3)	1773.06 (10)
Z	4
ρ_{calcd} (g cm^{-3})	1.321
μ (mm^{-1})	0.304
radiation (λ [Å])	graphite-monochromated Mo Kα (0.71073)
temperature (°C)	–100
scan type	ω scans (0.3°) (15 s exposures)
data collection 2Θ limit (deg)	55.02
total data collected	14660 ($-11 \le h \le 11$, $-15 \le k \le 15$, $-22 \le l \le 22$)
independent reflections	2038 (R_{int} = 0.0173)
number of observed reflections (*NO*)	1841 [$F_o^2 \ge 2\sigma(F_o^2)$]
structure solution method	direct methods (*SHELXD*)
refinement method	full-matrix least-squares on F^2 (*SHELXL–97*)
absorption correction method	Gaussian integration (face-indexed)
range of transmission factors	0.9313–0.8918
data/restraints/parameters	2038 / 0 / 117
goodness-of-fit (*S*) [all data]	1.068
final *R* indices[a]	
R_1 [$F_o^2 \ge 2\sigma(F_o^2)$]	0.0284
wR_2 [all data]	0.0788

[a] $R_1 = \Sigma||F_o| - |F_c||/ \Sigma |F_o|$; $wR_2 = [\Sigma w(F_o^2 - F_c^2)^2/ \Sigma w(F_o^4)]^{1/2}$.

Table 2 Selected details of the X-ray crystallographic structure of ligand **1b**.[a]

Interatomic Distances		
	S-C10	1.8402(13) Å
	S-C11	1.7714(12) Å
	N-C12	1.3733(17) Å
Bond angles		
	C10-S-C11	101.92(5)°
	S-C10-C1	109.66(8)°
Torsion angles		
	C11-S-C10-C1	–161.66(8)°
	C10-S-C11-C12	–78.72(10)°
	S-C11-C12-N	8.27(16)°
	C10-C1-C1'-C10'	–2.0(2)°

[a] More information available in Supplementary Information document.

The interatomic sulfur-sulfur distance (S-S') is 4.6405 Å and the bond angle of the thioether group (C10-S-C11) is 101.9° which lies in the expected range of alkyl-aryl thioethers. All three aromatic ring systems are planar with only minimal deviation of the planarity that are less that 1.18° when analyzing torsion angles of any 4 C atoms within each ring. In comparison to central xylene ring, both *ortho*-aminothiophenol pendants are tilted 28.95°. The amine groups are pointing outwards and are slightly bent downwards out of the aromatic ring plane due to steric or electronic interactions with the adjacent sulfur atom based on the torsion angle of S-C11-C12-N of 8.26°. The relative angles of both *ortho*-aminothiophenol pendants planes are not coplanar as they are bent downwards approximately 9° to 10°. The theoretical S-S' distance can vary from 1.0 Å to 5.9 Å based on geometric spatial cones of the S atom positions after the rotation of the C1-C10 and C1'-C10' bonds. This flexibility makes **1b** very versatile to adjust to the appropriate bite angle of *S,S'* chelation and *N,S*-M to M-*N,S* in binuclear complexes.

Ruthenium Complexes

Based on a modified synthetic procedure reported by Hamaker[50], a series of new η^6-arene ruthenium complexes (**2a-c**) were prepared by reacting equimolar amounts of $[Ru(\eta^6\text{-}p\text{-cymene})Cl_2]_2$, the corresponding N_2S_2-ligand (**1a-c**) and NaX salts (X = BF_4 or PF_6) (Scheme 1). The N_2S_2-ligands are ideal bridging template ligands to investigate the structures and properties of different Ru-Ru distances within the resulting binuclear N_2S_2-Ru_2 complexes as the central xylylene moiety forces the pendant *N,S*-chelate subunits into small, medium and large spacing depending on the substitution pattern. We suggest the use of the term 'hinged binuclear complexes' to describe compounds **2a-c** contrasting them with other types of binuclear complexes such as dimeric structures involving small bridging ligands, A-frame type systems and macrocyclic complexes. This does not preclude formation of metal-metal bonds or small ligand molecule bridges but ensures, when such bonds are broken, that one complex with two metal centres continues to exist as one entity as tethered *bis*-chelates. BF_4^- and PF_6^- anions were chosen for substitution of the chloride anion in order to stabilize the cationic moieties and to promote the growth of crystals for single crystal X-ray diffractrometry. The yields of the Ru complexes were good (64% to 85%), except for the *meta*-xylylene hinged Ru complex **2b** (10%) obtained from the BF_4^- reaction in which a mononuclear Ru complex (**3**) formed preferentially (~50% yield). CHN elemental analyses were congruent with theoretical yields for **2a-c** and were supplemented by Ru content measurements using inductively coupled plasma mass spectrometry (ICP-MS). ICP-MS analysis confirmed the presence of two Ru atoms per cation with a theoretical value of 22.61 wt% Ru compared to the experimental values of 22.65 ± 0.91 wt% (**2a**, X = BF_4), 22.31 ± 0.89 (**2c**, X = BF_4) and 23.79 ± 0.95 wt% (**2c**, X = PF_6). Mononuclear Ru complex **3** had a slightly higher value of 18.46 ± 0.73 wt% from the theoretical value of 16.22

wt% as the compound contains a small amount of diruthenium complex **2b** increasing the Ru content. Ruthenium and diruthenium content is also evident by the respective characteristic isotopic patterns in TOF HRMS analysis (see below). IR analysis of the ruthenium complexes showed the characteristic vibrations of ν_{NH} of the aniline group with a broad band at 3430 cm^{-1} and relatively sharp ν_{CH} bands at 2960 and 2870 cm^{-1} from the N_2S_2 backbone and cymene ligands. The fingerprint region of 1,500 cm^{-1} to 400 cm^{-1} had sharp and intense bands typical for aromatic rings. The counterion BF_4^- and PF_6^- salts are easily recognized by their respective very strong absorption band at 1080 cm^{-1} and 842 cm^{-1}. We were unable to assign a vibration band for a Ru-S bond in complex **3** due to obstruction by aromatic CC vibrations in the finger print region. UV-vis spectra of all Ru complexes had a strong absorption in the UV region with maxima at 230 nm for all complexes and shoulders at 260 nm corresponding to the aromatic ring systems. There was an extended low intensity absorption band from the UV region to 500 nm for all complexes. In mononuclear Ru complex **3** we observed an additional maximum at 440 nm which we tentatively assign to the *S,S'*-Ru complexation as this maximum is not observed with **2a-c**. We then focused on NMR and HRMS studies to determine the structures of the Ru complexes.

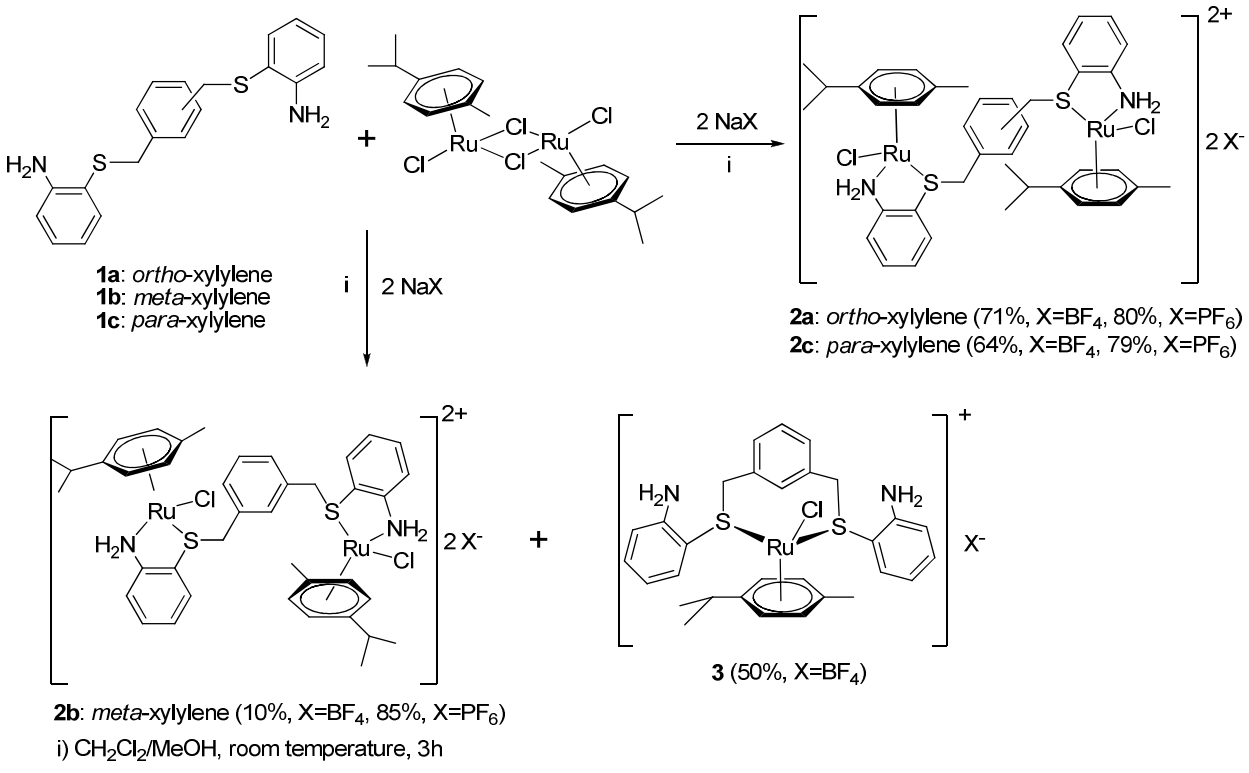

Scheme 1 Overview of Ru complex synthesis.

Ortho-xylene system

The light-brown coloured Ru_2 complex **2a** was obtained in 76% (X = BF_4) and 80% (X = PF_6) yield. We employed high resolution mass spectrometry using positive electrospray ionization. The parent ion isotope envelope of **2a** is located at 893 *m/z* corresponding to $[M-1]^+$, $C_{40}H_{47}Cl_2N_2Ru_2S_2$ (Fig. 3).‡ A loss of HCl and a cymene ligand resulted in mass fragments 857 *m/z* and 719 *m/z*, respectively. The base signal at 703 *m/z* was obtained on the loss of two HCl and cymene fragments and the capture of oxygen as an oxo, hydroxy or aquo ligand. We believe that the bridge motifs, Ru-O-Ru or Ru-OH-Ru, are likely species as we also observed the analogous mono-chloro mass fragment at 719 *m/z*. Mass fragment 703 *m/z* is detected in much

smaller abundances from the isomeric *meta*-xylylene ligand Ru_2 mass fragment of **2b** while there was no trace in spectrum of the *para*-xylylene complex **2c**. This demonstrates that a bridging species is formed with the closely spaced Ru-Ru of complex **2a**, while difficult with *meta*-xylylene hinged N_2S_2 ligand (**1b**) and impossible for the *para*-xylylene hinged N_2S_2 ligand (**1c**); a terminal Ru=O species is ruled out as it should have been observed in all three isomers **2a-c**. The mass fragments 623 *m/z* ($C_{30}H_{34}ClN_2RuS_2$) and 587 *m/z* ($C_{30}H_{32}N_2RuS_2$) are the singly bound η^6-cymene Ru (plus a Cl for 623 *m/z*) to **1a**, but we cannot distinguish whether the η^6-cymene Ru half sandwich is chelated through *N,S* or *S,S'*. Mass compound 462 *m/z* ($C_{24}H_{26}NRuS$) lost an *ortho*-aminothiophenol unit by cleavage of the CH_2-S bond. Mass fragment 359 *m/z* – particularly dominant when ionization in the mass spectrometer occurred under harsher conditions – is explained by CH_2-S cleavage of ligand **1a**. Under higher energy ionization conditions, the mass fragments assigned to $[\eta^6$-cymene Ru $(C_6H_4)]^+$ (312 *m/z*),$[\eta^6$-cymene $RuCl]^+$ (270 *m/z*) and $[\eta^6$-cymene $Ru]^+$ (235 *m/z*) are also observed. Despite high energy ionization condition, we were able to detect traces of the parent ion at 893 *m/z*.

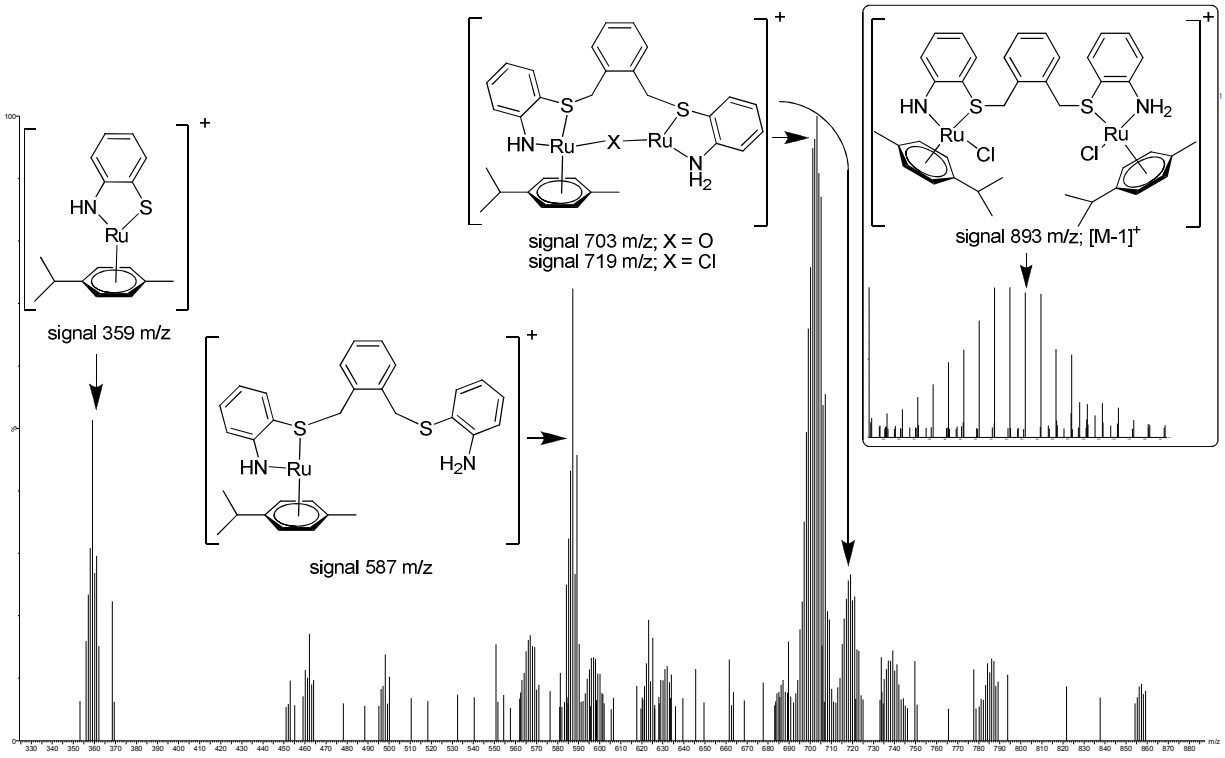

Fig. 3 MS analysis of **2a** (X = BF_4, PF_6) with proposed structures of the parent ion signal (inset) and the main mass fragments.

We used NMR spectroscopy for detailed structural characterization of the Ru_2 complex (**2a**) (Fig. 4). The ^{1}H NMR spectrum of **2a** (CD_2Cl_2) showed the presence of two different species in solution of which one exhibited dynamic behaviour at room temperature evidenced by the presence of sharp and broad proton resonance signals. The signals of the cymene ligand were used as internal reference showing a 1:1 ratio of the two species. The coordination of the N_2S_2-ligand was corroborated by the diastereotopic CH_2 protons ($H^{7,7'}$) in the backbone with a broad signal centred at 4.18 ppm and a doublet of doublets at 3.99 ppm and 4.09 ppm with coupling $^2J_{HH}$ of 12.8 Hz, which is in the expected range of germinal methylene protons. The

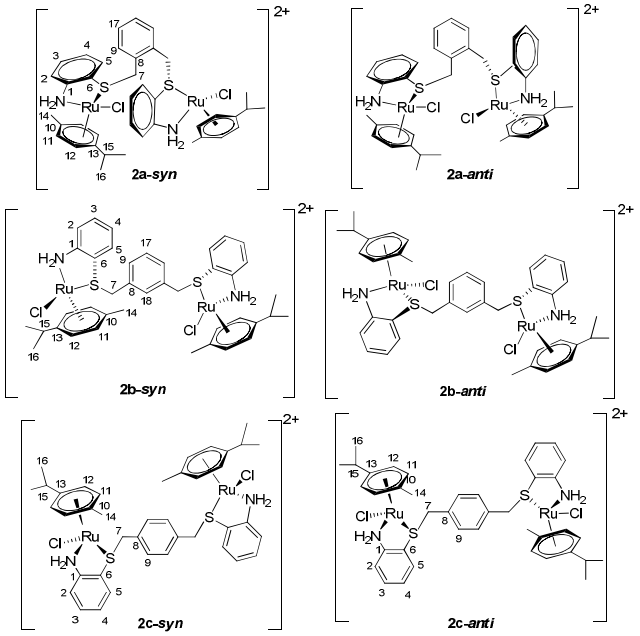

Fig. 4 Diastereomers of cationic Ru_2 complexes **2a-c** (X = BF_4, PF_6); atom positions simplified for clarity.

complexation of two η^6-arene Ru centres to both *N,S* chelates produced two sets of diastereomers, in racemic proportions, for a *syn* and *anti* configuration, labeled **2a-*syn*** and **2a-*anti*** (Fig. 4). We propose that the diastereomer that produced all the sharp resonances corresponds to **2a-*syn*** due to restricted flexibility. The cymene isopropyl methyl groups ($H^{16,16'}$) show three resonances at 0.96 ppm, 1.03 ppm and 1.14 ppm with characteristic doublet splitting. The signal at 1.03 ppm has twice the integration of the other signals and correlates to **2a-*syn*** as this is a *meso* compound with C_S symmetry. Signals 0.96 ppm and 1.14 ppm correlate to **2a-*anti***, but we cannot assign the Ru centre to which each belongs. Two other distinct resonances were observed for the NH_2 groups of **2a-*syn*** at 5.23 ppm and 8.32 ppm with $^2J_{HH}$ of 12.8 Hz. These two chemical shifts were unambiguously confirmed by absence of HSQC signals. The significant

difference in the chemical shift of the amine protons is due to a certain degree of interaction of one of the amine protons with the metal centre, shifting it upfield while the other proton is pointed away from the metal. The other set of NH_2 protons are broad signals at 5.85 ppm and 9.17 ppm referring to **2a-*anti*.** In addition, there is significant ^{1}H NMR signal overlap in the aromatic region, which we were able to resolve by comparison with the free ligand.[45] We see evidence in one of the amino-thioether moieties of interaction of the aromatic ring with the other Ru centre making the aromatic rings non-equivalent.

The ^{13}C jmod NMR spectrum of **2a** (CD_2Cl_2) shows evidence of the presence of two different species as well. Two sets of resonances were observed for each carbon of the cymene ligand at 84.7 ppm and 84.8 ppm ($C^{12,12'}$), 85.6 ppm and 85.8 ppm ($C^{11,11'}$), 100.1 ppm and 102.2 ppm ($C^{10,10'}$), and 108.9 ppm and 109.9 ppm ($C^{13,13'}$) with the exception of the resonance for the *C*-NH_2 (C^1) that showed only one signal at 145.1 ppm, presumably the overlap of both diastereomers. The other ipso carbons gave signals at 128.1 ppm and 129.2 ppm ($C^{6,6'}$) and 133.8 ppm and 134.1 ppm ($C^{8,8'}$) for the *anti* and *syn* diastereomers, respectively. While we were able to identify **2a-*syn*** and **2a-*anti***, we were not able to completely resolve the full NMR spectrum for each diastereomer due to signal overlap. The complexes are temperature sensitive and when the sample temperature was elevated evidence of decomposition was observed. Isolation of diastereomers is difficult as terminally bound thioether metal complexes undergo an intramolecular pyramidal inversion process with an associated low energy barrier of about 10 to 15 kcal/mol.[54]

206 ***Para*-xylene system**

207 The reaction of the *para*-xylylene hinged ligand **1c** with the ruthenium cymene dimer
208 forms the light-brown coloured, binuclear Ru complex **2c** as product for BF_4 (70%) and PF_6
209 (79%). The mass spectra of **2c** for both salts are identical and comparable to the structural isomer
210 complex **2a**. The parent ion signal, $[M-1]^+$, at 893 *m/z* was detected albeit in very low abundance.
211 The highest mass signal with significant abundance is 821 *m/z* of the *bis*-coordinated (η^6-cymene
212 Ru) to **1c** through loss of two HCl from $[M-1]^+$. 719 *m/z* and 703 *m/z* were not detected for **2c**.
213 The lack of these mass fragments supports the structure of the Ru_2 dimer complex that
214 geometrically disallows the formation of bridged Ru-Cl-Ru and Ru-O(H)-Ru structures as the
215 central *para*-xylylene ring forces the *ortho*-aminothiophenol pendants too far apart – even
216 though the methylene backbone link has some intrinsic flexibility. The next significantly
217 abundant mass species is 587 *m/z* corresponding to a single bound η^6-cymene Ru to the ligand
218 **1c**. The base peak is 359 *m/z* of the CH_2-S cleaved compound [η^6-cymene Ru (C_6H_4NS)]$^+$. Under
219 harsher ionization conditions, a more fragmented mass spectrum of **2c** was obtained as expected.
220 The base signal is 359 *m/z* and the next two abundant mass fragments are 312 *m/z* and 270 *m/z*
221 which are η^6-cymene Ru species complexed to Cl and benzene.

222 Based on ^{1}H NMR spectroscopy results, **2c** is similar to the results previously described
223 with complex **2a**, evidencing the presence of the *syn* and *anti* isomers of **2c** (Fig. 4) in the ratio
224 of 1:1. We propose that the Ru centres are too far apart to have any influence on preference for
225 any diastereomer, hence producing a statistical equimolar ratio. We do not see significant
226 broadening of one isomer as seen with **2a** as both diastereomers of **2c** are flexible with little
227 restrictions. We observe a clear set of two isomers for all ^{1}H resonances with particularly strong
228 chemical shifts for the methyl signals of the isopropyl cymene ($H^{16,16'}$) at 1.08 ppm and 1.83 ppm

coupling to the respective, overlapping isopropyl protons at 2.74 ppm with $^{3}J_{HH}$ of 6.8 Hz. The methylene protons ($H^{7,7'}$) show the characteristic geminal coupling pattern of a set of doublets, with $^{2}J_{HH}$ of 8.4 Hz with 4.15 ppm and 4.83 ppm as well as 4.18 ppm and 4.77 ppm. The ^{1}H splitting on the resonances for the NH_2 groups also show doublets at 5.10 ppm ($^{2}J_{HH}$ = 11.4 Hz) and 8.24 ppm ($^{2}J_{HH}$ = 11.4 Hz) while no broadening is observed as in **2a**. The coordination of the *N,S*-ligand produces a non-equivalent arene resulting in two sets of proton resonance signals for $H^{16,16'}$ at 1.07 ppm and 1.83 ppm as doublets with couplings of 6.8 Hz as well as two distinct chemical shifts for methyl protons ($H^{14,14'}$) at 2.05 ppm and 2.06 ppm. However, the chemical shift of the isopropyl proton ($H^{15,15'}$) at 2.73 ppm was minimally affected by the diastereomeric environment producing a signal overlap. Strong resonances of the characteristic methylene groups in the xylylene backbone in the $^{13}C\{^{1}H\}$ NMR spectrum shows the presence of the two diastereomers, **2c-*syn*** and **2c-*anti***.

***Meta*-xylene system**

The reaction of the *meta*-xylene bridged ligand **1b**, $[Ru(\eta^{6}\text{-}p\text{-cymene})Cl_2]_2$ and $NaPF_6$ produced the expected binuclear Ru complex **2b** in 87% yield. The Ru_2 complex was isolated as a light-brown solid from the reaction mixture by precipitation through addition of diethyl ether. **2b** (X = BF_4 and PF_6) was analyzed by HRMS. The $[M\text{-}1]^{+}$ signal and other mass fragments were congruent with the structural isomers of **2a**,**c**. Two diastereomers of **2b** were observed in the ^{1}H NMR spectrum (Fig. 4). These two species, **2b-*syn*** and **2b-*anti***, occurred in a 2:1 ratio based on cymene group integrations. We assign the minor component as **2b-*anti*** since it also shows signal broadening due to fluxional behaviour. The methylene ($H^{7,7'}$) protons along the backbone of the ligand produce two sharp doublets for the most abundant isomer centred at 4.07 ppm and 4.92 ppm with a *J*-coupling of 11.2 Hz and two doublets, which have a broadened shape, centred at

4.20 ppm and 4.61 ppm with *J*-coupling of 10.4 Hz. The coordination of the NH_2 moiety is evidenced by two sets of resonances 5.08 ppm and 8.22 ppm with a 10.0 Hz coupling and 5.16 ppm and 8.48 ppm for the second diastereomer with a more broadened 10 Hz coupling. With **2b**, we see no interaction of the aromatic rings with the Ru centre as was observed in **2a**. The $^{13}C\{^1H\}$ NMR spectrum also displayed the presence of two diastereomers. Two set of resonances are observed for the methylene carbon at 42.5 ppm and 42.9 ppm. The *ipso* carbons of the isopropyl group in the cymene ligand are 103.5 ppm and 103.7 ppm and the isopropyl C centre was 109.1 ppm and 109.6 ppm. Additionally, the quaternary carbons are observed at 129.0 ppm and 129.1 ppm for $C^{8,8'}$, 134.5 ppm and 134.8 ppm for $C^{6,6'}$, and with $C^{1,1'}$ at 143.8 ppm and 144.2 ppm.

When the reaction of **1b** and $[Ru(\eta^6\text{-}p\text{-cymene})Cl_2]_2$ was carried out in the presence $NaBF_4$, a dark brown solid, insoluble in common organic solvents with exception of the strong aprotic, polar solvents DMSO and DMF, was obtained after the addition of diethyl ether. After filtration, a second fraction precipitated from the organic solvent phase. The different reactivity of the BF_4^- salt with ligand **1b** was unexpected as reactions of **1a** and **1c** have resulted in similar yields, MS and NMR data for both $NaBF_4$ and $NaPF_6$. With $NaBF_4$, we observed in the 1st fraction the presence of the mononuclear Ru complex (**3**) in approximately 50% yield as a main product in a mixture with the binuclear complex **2b**. The second fraction contained the binuclear Ru complex **2b** in about 10% yield. An unidentified Ru-arene complex and free cymene were obtained as by-products. Compound **3** was obtained only as the BF_4 salt; the precipitate with PF_6 as counterion was not observed. The MS and NMR data of **2b** are congruent for BF_4 and PF_6 counter anions. Using HRMS, we were able to identify compound **3** as a mono-ruthenium

complex with the parent ion at 623 *m/z* and a base signal of 587 *m/z* corresponding to loss of HCl. **3** occurs as a mixture of diastereomers.

We detected two distinct signals in the LC chromatogram of the 1st fraction. At first glance, those MS spectra look similar but there is a profound distinction between Ru_2 complex **2b** and mono-ruthenium complex **3**. The characteristic mass fragments containing two Ru centres can only be found with the analyte eluded at 0.26 min. A search for these Ru_2 entities in the signal eluted at 0.20 min provides only background noise. The mono-ruthenium complex **3** is much smaller than the Ru_2 species **2b** and the reduced surface interaction of the non-polar C-18 column causes it to elude first and allows the identification of the $[(\eta^6\text{-cymene})Ru\ \mathbf{1b}]^+$ mass fragment at 587 *m/z* from **3** and not from **2b**.

NMR analysis was conducted in DMSO-d_6 as the product was not soluble in CD_2Cl_2. The ^1H NMR spectrum showed a complicated mixture of species in solution with **2b** and **3** as the main components. After 16 h at room temperature, the major component was the monometallic complex **3**, and according to the mass spectrometry results, the minor component in the mixture corresponds to the Ru_2 complex **2b** which also precipitated from the DMSO-d_6 solution. We detected an approximate 3:1 ratio of **3-*syn*** to **3-*anti***. **3-*syn*** is the major compound as we postulate that the aniline pendants can pull backwards allowing a greater degree of rotation of the cymene compared to **3-*anti*** (Fig. 5). **3-*syn*** is a *meso* compound with simplified signals resulting from symmetry but identification of the minor compound was only partially possible due to small and overlapping signals. We were able to characterize that the isopropyl signals 1.30 ppm ($H^{16'}$), singlet 1.93 ppm ($H^{14'}$) and the septet of $H^{15'}$ at 2.63 ppm belong to **3-*anti***. Due to its symmetry, broad singlet signals at 3.90 ppm and 4.09 ppm are observed for the methylene protons. Resolution of those signals through low temperature NMR experiments was not possible

due to the limitations of DMSO-d_6. There is no coordination of the NH_2 groups to Ru as observed with the binuclear Ru complexes because only a broad resonance appears at 3.52 ppm without coupling. For the main product in the mixture, it is proposed that both S atoms in the ligand are coordinated to the η^6-cymene Ru moiety. The central C*H* aromatic of **1b** appeared as a multiplet at 6.51 ppm for **3-*anti*** and as a doublet at 6.77 ppm for **3-*syn***. In the $^{13}C\{^1H\}$ NMR spectrum (DMSO-d_6) the resonances for these *C*H_2-S appear at 37.2 ppm for **3-*syn*** and 37.6 for **3-*anti***. The structure of compound **3** gives rise to the possibility of the formation of the corresponding pincer Ru complex formed by a cyclometallation reaction. To our knowledge, this would be the first *SCS* pincer complex for Ru. Cyclometallation for SCS pincer complexes of Pd is known[55-58] and we have isolated the related Pd complexes[59] of **1a-c**. We attempted to facilitate the cyclometallation reaction of activation of the C-H of *meta*-xylene (**3**) in the DMSO-d_6 solution by heating to 50 °C but no reaction was observed in the ^1H NMR even after 3 days. When the temperature was increased to 100 °C, the complex decomposed and free cymene was observed.

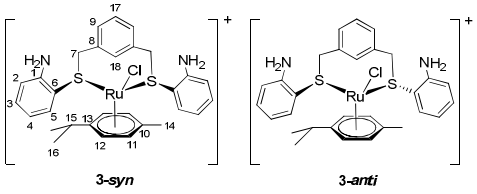

Fig. 5 Diastereomers of cationic mono-ruthenium complex **3** (X = BF_4).

Conclusion

The series of *ortho-, meta-* and *para*-xylylene *bis*-(*o*-aminothiophenol) N_2S_2 ligands readily form hinged binuclear Ru complexes with η^6-cymene as BF_4 and PF_6 salts. The η^6-cymene Ru centres are complexed to the tetradentate ligands as *bis-N,S* chelates of the *o*-aminothiophenol pendants and generate racemic sets of *syn* and *anti* configuration diastereomers. With the *ortho-* and *meta*-hinged ligands, the less sterically hindered *anti* diastereomer is favoured to the *syn* isomer. When using these complexes (**2a-c**) as precatalysts for Ru based catalysis, one must consider that the diastereomers can have different activities and that isolation of the diastereomers may be practically impossible based on inversion at the S donor atoms. The *meta*-xylylene hinged ligand **1b** exhibited different reactivity behaviour in the presence of $NaBF_4$ and $NaPF_6$. We postulate that the formation of the mononuclear Ru complex **3** (*syn* and *anti* diastereomers) is favoured in the presence of a small non-coordinating anion resulting in a coordinative shift of *N,S*-chelation to *S,S'*-chelation instead. Such coordination is only supported with **1b** having the appropriate donor atoms spacing. Further research is required to gain further understanding of the mechanism of this complexation reaction. The resulting *S,S'*-Ru (η^6-cymene) cation can be used as precursor of potential *SCS* pincers involving Ru. The Ru complexes will also be investigated for electrochemical studies and as catalysts for alkene metathesis and hydrogenation reactions.

Experimental

All solvents and chemicals (reagent grade) for synthesis were purchased from commercial sources (Sigma-Aldrich, Fisher Scientific and Strem Chemicals) and were used without further purification. UPLC solvents were Optima ® grade obtained from Fisher Scientific. Ligands **1a-c** were synthesized according to the procedure previously reported.[45] X-ray structure of **1b** was

deposited with the Cambridge Crystallographic Data Centre (CCDC 967363). $NaPF_6$ was dissolved in MeOH. $NaBF_4$ was dispersed in MeOH and H_2O was added dropwise until the salt was completely dissolved. NMR spectra were recorded on a 400 MHz Bruker Avance II spectrometer operating at 400.17 MHz for ^1H and 100.6 MHz for ^{13}C. $^1H/^{13}C$ NMR chemical shifts are reported in ppm and referenced to tetramethylsilane (δ = 0 ppm) or residual solvent signal (CD_2Cl_2 δ = 5.32 ppm/ 54.0 ppm; DMSO-d_6 δ = 2.49 ppm/ 39.7 ppm) as internal standard. *J* values are given in Hz. Assignment of diastereotopic signals is indicated by apostrophe (‘) and overlapping signals are indicated by asterisk (*). UPLC-HRMS analyses were performed on a Waters Acquity Xevo G2 QToF using a C-18 column (Waters BEH C18 1.7 µm, 2.1 mm × 50 mm) and ESI positive mode. Compounds were dissolved in 90 Vol% CH_3CN : 10 Vol% nanopure H_2O for UPLC-HRMS analysis. Calculated theoretical isotope envelope for $[M-1]^+$ of **2a-c** isomers is listed only under **2a**. MS fragmentation results are provided for major signals of isotopic pattern envelope and rounded to 0.1 *m/z* for signals greater than 10% of height of base signal. MS analyses of **2a-c** are reported herein for one counterion as results were congruent for X = BF_4, PF_6, respectively. Elemental analysis (CHN) was conducted by MHW Labs, Phoenix, Arizona, US. UV-vis spectra were recorded in quartz cuvettes on a Varian Cary 100 Bio UV-Vis spectrometer. ε was not determined for **3** due to mixture with **2b** (X= PF_6). FTIR spectra were recorded on a Thermo Nicolet 6700 FTIR Spectrometer as KBr pellet (approximately 1.5 mg compound in 300 mg anhydrous KBr) in the 4,000 cm^{-1} to 400 cm^{-1} range with 2 cm^{-1} resolution. ICP-MS analysis was performed using an PerkinElmer ICP-MS NexION 300D on Ru (mass 102 amu) and samples in the range of 300 ppb in a 1 wt% HNO_3 solution (50 mL) containing less than 1 wt% DMSO. Calibration was conducted with $[Ru(\eta^6\text{-}p\text{-cymene})Cl_2]_2$ in the range of 100 to 500 ppb with EtOH substituting for DMSO. ICP- results are the averages of duplicate runs and

the measurement error is estimated to ± 4% based on measurement error, purity of calibration standard and sample preparation.

Synthesis

$[Ru_2(\eta^6\text{-}p\text{-cymene})_2(1a)]X_2$ (X = BF_4, PF_6), 2a. In a 10 mL screwtop vial, a solution of **1a** (57.5 mg, 0.16 mmol) in 3 mL CH_2Cl_2 was added to a solution of $[Ru(\eta^6\text{-}p\text{-cymene})Cl_2]_2$ (100 mg, 0.16 mmol) dissolved in 2 mL CH_2Cl_2. Immediately, the reaction mixture turned from red to brown. After stirring for 15 min at room temperature, $NaBF_4$ (15.6 mg, 0.32 mmol) in 2 mL MeOH/H_2O was added and allowed to stir for 3 h (for $NaPF_6$ (54.7 mg, 0.32 mmol) in 2 mL MeOH). The reaction was quenched with H_2O (3 mL) and vigorously stirred for 5 min in order to remove NaCl and excess NaX. The aqueous phase was removed and diethyl ether (20 mL) was added to the organic phase. The resulting precipitate was then isolated by filtration and dried in vacuum for 3 h yielding a light orange powder (122.6 mg, 71% yield for X = BF_4; 135.2 mg, 80% yield X = PF_6). ^{1}H NMR (400 MHz, CD_2Cl_2): δ = 0.96 (d, 6H, H^{16}, $^3J_{HH}$ = 6.8 Hz), 1.03 (d, 12H, $H^{16'}$, $^3J_{HH}$ = 7.2 Hz), 1.14 (d, 6H, $C^{16''}$, $^3J_{HH}$ = 6.8 Hz), 1.87* (broad s, 3H, C^{14}), 2.07 (s, 3H, $C^{14'}$), 2.64* (broad sept, 2H, C^{14}, $^3J_{HH}$ = 7.2 Hz), 2.69* (sept, 2H, $C^{14'}$, $^3J_{HH}$ = 6.8 Hz), 3.99 (d, 2H, H^7, $^2J_{HH}$ = 12.8 Hz), 4.09 (d, 2H, H^7, $^2J_{HH}$ = 12.8 Hz), 4.18 (b, 2H, $H^{7'}$), 5.23 (d, 1H, N*H*H, $^2J_{HH}$ = 12.8 Hz), 5.50* (m, 2H, H^{12}), 5.56* (m, 2H, $H^{12'}$), 5.82* (m, 2H, H^{11}), 5.85 (b, 2H, NH_2') 6.74 (d, 2H, H^2, $^3J_{HH}$ = 8.0 Hz), 7.11 (t, 2H, H^3, $^3J_{HH}$ = 7.6 Hz), 7.42* (m, 2H, $H^{3'}$), 7.44* (m, 2H, H^4), 7.46* (m, 2H, H^{17}), 7.51 (m, 2H, $H^{17'}$), 7.65 (m, 2H, H^9), 7.72 (d, 2H, H^5, $^3J_{HH}$ = 7.6 Hz), 7.76 (m, 2H, $H^{9'}$), 7.78* (d, 2H, $H^{5'}$, $^3J_{HH}$ = 7.6 Hz), 8.32 (d, 2 H, NH*H*, $^2J_{HH}$ = 12.8 Hz), 9.17 (b, 1H, NH_2'). $^{13}C\{^1H\}$ NMR (100.6 MHz, CD_2Cl_2): δ = 18.8 (C^{14}), 21.8 (C^{16}), 22.6 ($C^{16'}$),

31.2 (C^{15}), 40.7 (C^{7}), 84.7 (C^{12}), 84.8 ($C^{12'}$), 85.8 (C^{11}), 87.6 ($C^{11'}$), 100.1 (C^{10}), 102.2 ($C^{10'}$), 108.9 (C^{13}), 109.9 ($C^{13'}$), 128.0 (C^{8}), 128.1 (C^{5}), 128.6($C^{5'}$), 129.0 (C^{3}), 129.2 ($C^{8'}$), 130.5 ($C^{3'}$), 130.8 (C^{17}), 131.7 (C^{9}), 131.9 (C^{17}), 132.0 (C^{4}), 132.3 (C^{2}), 133.5 ($C^{2'}$), 133.8 (C^{6}), 134.1 ($C^{6'}$), 145.1 (C^{1}). Elemental analysis (%) calcd. for $C_{40}H_{48}B_2Cl_2F_8N_2Ru_2S_2$ (1067.61): C, 45.00; H, 4.53; N, 2.62. Found: C, 44.89; H, 4.61; N, 2.55. ICP-MS calcd. for $C_{40}H_{48}Cl_2N_2Ru_2S_2$: 22.61 wt% Ru. Found: 22.65 ± 0.91 wt% Ru for **2a** (X = BF_4). HRMS for $[M-1]^+$ (X = BF_4) calc. 898.0656 (25%), 897.0641 (55), 896.0655 (55), 895.0648 (90), 894.0655 (85), 893.0653 (100), 892.0659 (90), 891.0659 (75), 890.0666 (60), 889.0668 (45), 888.0676 (25). Found: 898.0596 (30%), 897.0642 (70), 896.0694 (65), 895.0628 (100), 894.0690 (85), 893.0635 (97), 892.0648 (95), 891.0604 (80), 890.0689 (65), 889.0657 (45), 888.0753 (30). MS (X = PF_6; ESI low energy, *m/z*) 893.1 (<1%), 857.3 (10), 786.2 (15), 730.1 (15), 719.1 (28), 703.1 (100), 623.2 (20), 587.2 (70), 498 (12), 462.2 (15), 359.1 (50). λ_{max}/nm for **2a** (X = BF_4, CH_2Cl_2) 230 (ε/dm^3 mol^{-1} cm^{-1} 81 500) and 260 (sh). IR (**2a**, X = BF_4, KBr) 3422, 3225, 3060, 2965, 1603, 1585, 1477, 1447, 1389, 1306, 1282, 1080, 1050, 877, 822, 765 cm^{-1}.

[Ru_2(η^6-*p*-cymene)$_2$(1b)](PF_6)$_2$, 2b. Following the procedure described for **2a**, [Ru(η^6-*p*-cymene)Cl_2]$_2$ (100 mg, 0.16 mmol), **1b** (57.5 mg, 0.16 mmol) yielded light brown solid (148.3 mg, 85% yield. ^{1}H NMR (400 MHz, CD_2Cl_2): δ = 1.05 (d, 6H, H^{16}, $^3J_{HH}$ = 6.8 Hz), 1.13 (d, 3H, $H^{16'}$, $^3J_{HH}$ = 6.8 Hz), 1.31 (d, 3H, $^3J_{HH}$ = 6.8 Hz), 2.04 (s, 3H, H^{14}), 2.07 (s, 3H, $H^{14'}$), 2.75* (sept, 2 x 1H, $H^{15,15'}$, $^3J_{HH}$ = 6.8 Hz), 4.07 (d, 2H, H^{7}, $^2J_{HH}$ = 11.2 Hz), 4.20 (d, 2H, $H^{7'}$, $^2J_{HH}$ = 10.4 Hz), 4.61 (d, 2H, $H^{7''}$, $^2J_{HH}$ = 10.4 Hz,), 4.92 (d, 2H, $H^{7'''}$, $^2J_{HH}$ = 11.2 Hz), 5.08 (d, 2H, N*H*H, $^2J_{HH}$ = = 9.6 Hz), 5.16 (d, 2H, N*H'*H, $^2J_{HH}$ = 10.8 Hz), 5.44* (m, 4H, $H^{12,12'}$), 5.71* (d, 2H, H^{11}, $^3J_{HH}$ = 8.0 Hz), 5.77* (d, 2H, $H^{11'}$, $^3J_{HH}$ = 8.0 Hz), 7.37-7.72 (m, 10H, $H^{2,3,4,9,17,18}$), 8.22

(d, NH*H'*, $^{2}J_{HH}$ = 10.8 Hz), 8.47 (b, 2H, NH*H*). $^{13}C\{^{1}H\}$ NMR (100.6 MHz, CD_2Cl_2): δ =18.7 (C^{14}), 22.1 (C^{16}), 22.4 ($C^{16'}$), 31.2 (C^{15}), 42.5 (C^{7}), 42.9 ($C^{7'}$), 84.5 (C^{11}), 85.2 ($C^{11'}$), 85.3 (C^{12}), 85.6 ($C^{12'}$), 100.3 (C^{10}), 103.7 ($C^{10'}$), 109.0 (C^{13}), 109.2 ($C^{13'}$), 128.0 (C^{9}), 128.1 ($C^{9'}$), 129.0* (C^{8}), 129.1* ($C^{8'}$), 129.2 (C^{5}), 129.4 ($C^{5'}$), 129.9 (C^{17}), 130.2 (C^{18}), 131.7 (C^{3}), 131.8 ($C^{3'}$), 132.0 (C^{4}), 132.8 (C^{2}), 133.7 ($C^{2'}$), 134.5 (C^{6}), 134.8 ($C^{6'}$), 143.8 (C^{1}), 144.2 ($C^{1'}$). Elemental analysis (%) calcd. for $C_{40}H_{48}Cl_2F_{12}N_2P_2Ru_2S_2$ (1183.93): C, 40.58; H, 4.09; N, 2.37. Found: C, 40.73; H, 4.16; N, 2.28. HRMS for $[M-1]^{+}$ found: 898.0781 (20%), 897.0642 (55), 896.0632 (50), 895.0751 (90), 894.0690 (85), 893.0697 (100), 892.0648 (90), 891.0727 (90), 890.0628 (55), 889.0657 (50), 88.0569 (30). MS (ESI medium energy, *m/z*) 893.1 (<1%), 857.1 (3), 821.1 (5), 719.1 (5), 703.1 (1), 687.0 (10), 582.9 (10), 462.1 (7), 357.1 9100), 317.0 (15). λ_{max}/nm (DMF) 266 (ε/$dm^3mol^{-1}cm^{-1}$ 17 100), 303 (sh) and 439 (4 900). IR (KBr) 3425, 3064, 2967, 2876, 2381, 2348, 2316, 1628, 1605, 1557, 1475, 1446, 1124, 1080, 1058, 999, 870, 843, 804, 732 cm^{-1}.

$[Ru_2(\eta^6$-*p*-cymene)$_2$(1c)]X_2 (X = BF_4, PF_6), 2c. Following the procedure described for **2a**, $[Ru(\eta^6$-*p*-cymene)$Cl_2]_2$ (100 mg, 0.16 mmol), **1c** (57.5 mg, 0.16 mmol) yielded light brown solid (110.4 mg, 64% yield for X = BF_4; 134.3 mg, 79% yield for X = PF_6). ^{1}H NMR (400 MHz, CD_2Cl_2): δ = 1.08 (d, 6H, H^{16}, $^{3}J_{HH}$ = 6.8 Hz), 1.83 (d, 6H, H^{16}, $^{3}J_{HH}$ = 6.8 Hz), 2.05 (s, 3H, H^{14}), 2.06 (s, 3H, H^{14}), 2.73* (sept, 2 x 1H, H^{15}, $^{3}J_{HH}$ = 6.8 Hz), 4.15 (d, 1H, H^{7}, $^{2}J_{HH}$ = 8.4 Hz), 4.18 (d, 1H, $H^{7'}$, $^{2}J_{HH}$ = 8.4 Hz), 4.77 (d, 2H, $H^{7''}$, $^{2}J_{HH}$ = 8.4 Hz), 4.83 (d, 2H, $H^{7'''}$, $^{2}J_{HH}$ = 8.4 Hz), 5.12 (broad d, 1H, N*H*H, $^{2}J_{HH}$ =11.6 Hz), 5.36 (m, 4H, H^{11}), 5.54* (m, 2H, H^{12}), 5.55* (m, 2H, $H^{11'}$), 5.68 (m, 2H, $H^{12'}$), 7.38* (m, 4H, H^{5}), 7.40* (m, 4H, H^{4}), 7.52* (m, 4H, H^{3}), 7.54* (m, 4H, H^{2}), 7.68* (s, 4H, H^{9}), 7.69* (s, 4H, $H^{9'}$), 8.36 (broad d, NH*H*, $^{2}J_{HH}$ = 11.6 Hz). $^{13}C\{^{1}H\}$ NMR

(100.6 MHz, CD_2Cl_2): δ = 18.7 (C^{14}), 22.1 (C^{16}), 22.4 ($C^{16'}$), 31.2* (C^{15}), 42.6 (C^7), 42.7 ($C^{7'}$), 84.5 (C^{11}), 85.2 ($C^{11'}$), 85.3 (C^{12}), 85.5 ($C^{12'}$), 103.5 (C^{10}), 109.0 (C^{13}), 128.2 (C^5), 129.0 (C^8), 129.4 (C^3), 131.5 (C^2), 131.7 (C^9), 131.9 ($C^{9'}$), 132.0 (C^4), 134.6 (C^6), 143.6 (C^1), 143.7 ($C^{1'}$). Elemental analysis (%) calcd. for $C_{40}H_{48}B_2Cl_2F_8N_2Ru_2S_2$ (1067.61): C, 45.00; H, 4.53; N, 2.62. Found: C, 45.19; H, 4.87; N, 2.78. ICP-MS calcd. for $C_{40}H_{48}Cl_2N_2Ru_2S_2$: 22.61 wt% Ru. Found: 22.31 ± 0.89 wt% Ru (**2c**, X = BF_4) and 23.79 ± 0.95 wt% Ru (**2c**, X = PF_6). HRMS for $[M-1]^+$ (X = BF_4) found: 898.0323 (30%), 897.0244 (50), 896.0048 (70), 895.0103 (85), 894.0163 (90), 893.0106 (100), 892.0178 (90), 891.0133 (70), 890.0154 (65), 889.0120 (55), 887.9969 (30). MS (X = BF_4; ESI low energy, *m/z*) 893.1 (<1%), 587.1 (20), 462.1 (12), 359.0 (100), 312.0 (40), 270.1 (60). λ_{max}/nm for **2c** (X = BF_4, CH_2Cl_2) 231 (ε/dm^3 mol^{-1} cm^{-1} 53 200) and 278 (sh). λ_{max}/nm for **2c** (X = PF_6, CH_2Cl_2) 230 (ε/dm^3 mol^{-1} cm^{-1} 81 500), 270 (sh) and 312 (8 300). IR (**2c**, X = BF_4, KBr) 3435, 3234, 3062, 2965, 1606, 1556, 1503, 1477, 1389, 1282, 1080, 1050, 877, 764 cm^{-1}. IR (**2c**, X = PF_6, KBr) 3435, 3294, 3067, 2967, 1588, 1554, 1505, 1477, 1448, 1390, 1281, 1200, 1160, 1058, 1033, 842, 761, 740 cm^{-1}.

[Ru(η^6-*p*-cymene)$_2$(1b)Cl](BF$_4$), 3. Following the procedure described for **2a**, [Ru(η^6-*p*-cymene)Cl_2]$_2$ (100 mg, 0.16 mmol), **1b** (57.5 mg, 0.16 mmol) precipitated a dark brown powder upon addition of 20 mL Et_2O (63.3 mg, approx. 50%). The supernatant organic phase was further treated with Et_2O resulting in a light brown precipitate (17.0 mg, approx. 10%) assigned to **2b-BF$_4$** which has identical analytical data of NMR and MS as **2b-PF$_6$**. Analytical data for major compound **3** are listed here. ^{1}H NMR (400 MHz, DMSO-d_6): δ = 1.18 (d, 6H, H^{16}, $^3J_{HH}$ = 6.8 Hz), 2.08 (s, 3H, H^{14}), 2.82 (sept, 1H, H^{15}, $^3J_{HH}$ = 6.8 Hz), 3.52 (b, 2H, NH_2), 3.90 (broad singlet, 2H, H^7), 4.09 (broad singlet, 2H, $H^{7'}$), 5.77 (d, 2H, H^{12}, $^3J_{HH}$ = 6.4 Hz), 5.82 (d, 2H, H^{11},

449 $^{3}J_{HH}$ = 6.4 Hz), 6.51 (m, 1H, H^{17}), 6.77 (s, 1H, H^{18}), 7.02-7.18* (m, 4H, $H^{2,3,4,5}$), 7.43-7.52* (m,
450 3H, $H^{9,17}$), 8.50 (d, 2H, N*H*H, $^{2}J_{HH}$ = 13.6 Hz). $^{13}C\{^{1}H\}$ NMR (100.6 MHz, DMSO-d_6): δ = 17.8
451 (C^{14}), 21.5 (C^{16}), 29.9 (C^{15}), 37.2 and 37.6 (C^{7}), 85.5 (C^{12}), 86.3 (C^{11}), 100.2 (C^{10}), 106.7 (C^{13}),
452 114.8 (C^{18}), 127.5 (C^{5}), 128.1 (C^{8}), 129.2 (C^{9}), 129.5 (C^{4}), 130.6 (C^{17}), 131.1 (C^{2}), 134.7 (C^{3}),
453 138.5 (C^{6}), 148.6 (C^{1}). ICP-MS calcd. for $C_{40}H_{48}ClN_2RuS_2$: 16.22 wt% Ru. Found: 18.46 ± 0.73
454 wt% Ru. HRMS for M^{+} calc. 627.0883 (20%), 626.0917 (25), 625.0894 (80), 624.0908 (50),
455 623.0899 (100), 622.0907 (60), 621.0906 (40), 620.0914 (30). Found: 627.1953 (25%), 626.1990
456 (30), 625.1947 (80), 624.1950 (50), 623.1937 (100), 622.1945 (60), 621.1926 (40), 620.1934
457 (30). MS (ESI low energy, *m/z*) 623.2 (40%), 587.2 (100), 478.2 (35), 412.0 (30), 359.1 (20),
458 312.1 (35), 271.0 (20). λ_{max}/nm for **3** (DMF) 229, 270 and 440. IR (KBr) 3435, 3273, 3061,
459 2964, 2873, 1601, 1561, 1473, 1388, 1280, 1080, 1020, 870, 803, 763 cm^{-1}.

460

461 **Acknowledgements**

462 The authors thank NSERC, Canada Foundation for Innovation, NSRIT, Enterprise Cape Breton
463 Corporation and CBU for financial support. The assistance of J. MacInnis with UPLC-HRMS
464 experiments and Dr. R. Kaliaperumal, Verschuren Centre for Sustainability in Energy and the
465 Environment, with ICP-MS was greatly appreciated.

466 **Notes and references**

467 Electronic Supplementary Information (ESI) available.

468 ‡ Oxygen is available for this reaction as the complex was dissolved in a 90 Vol% : 10
469 Vol% acetonitrile : water solution in presence of 0.1 wt% formic acid for the UPLC-HRMS

analysis. The experimental results overlapped congruently with the theoretical isotope pattern and we were only able to detect singly charged complexes in absence of fractional *m/z* units of multiple charged species at 446 *m/z* or 298 *m/z*.

§ We were unable to obtain suitable crystalline material for X-ray structural analysis of the metal complexes. We have obtained material that appeared crystalline to the eye but did not diffract. We hypothesize that the lack of directed intermolecular forces such as H-bonding or dipole moments makes it difficult for the compounds to form suitable crystal packing. In addition, the large non-polar sphere of cymene and aromatic rings is little differentiated between the sets of diastereomers further complicating crystal stacking.

1. M. E. Broussard, B. Juma, S. G. Train, W.-J. Peng, S. A. Laneman and G. G. Stanley, *Science*, 1993, **260**, 1784-1786.
2. G. Süss-Fink, *Angew. Chem. Int. Engl.*, 1994, **33**, 67-69.
3. I. Yu, A. Acosta-Ramírez and P. Mehrkhodavandi, *J. Am. Chem. Soc.* 2012, **134**, 12758-12773.
4. M. R. Radlauer, M. W. Day and T. Agapie, *J. Am. Chem. Soc.* 2012, **134**, 1478-1481.
5. M. Shibasaki, M. Kanai, S. Matsunaga and N. Kumagai, *Acc. Chem. Res.* 2009, **42**, 1117-1127.
6. R. D. Adams and B. Captain, *Angew. Chem. Int. Ed.* 2008, **47**, 252-257.
7. A. Duschek and S. F. Kirsch, *Angew. Chem. Int. Ed.* 2008, **47**, 5703-5705.
8. S. Gambarotta and J. Scott, *Angew. Chem. Int. Ed.* 2004, **43**, 5298-5308.
9. S. Jautze and R. Peters, *Angew. Chem. Int. Ed.* 2008, **47**, 9284-9288.
10. Eds:, M. Shinasaki and Y. Yamamoto, *Multimetallic Catalysts in Organic Synthesis*, Wiley-VCH, Weinheim, 2005.
11. J. Xiao and R. J. Puddephatt, *Coord. Chem. Rev.* 1995, **143**, 457-500.
12. S. Sproules and K. Wieghardt, *Coord. Chem. Rev.* 2010, **254**, 1358-1382.

13. S. R. Presow, M. Ghosh, E. Bill, T. Weyhermuller and K. Wieghardt, *Inorg. Chim. Acta*, 2011, **374**, 226-239.
14. R. Martínez-Máñez and F. Sancenón, *Chem. Rev.* 2003, **103**, 4419-4476.
15. J. Perez and L. Riera, *Chem. Soc. Rev*, 2008, **37**, 2658-2667.
16. J. W. Steed, *Chem. Soc. Rev.* 2009, **38**, 506-519.
17. A. Kumar, S.-S. Sun and A. J. Lees, *Coord. Chem. Rev.* 2008, **252**, 922-939.
18. A. E. Hargrove, S. Nieto, T. Zhang, J. L. Sessler and E. V. Anslyn, *Chem. Rev.* 2011, **111**, 6603-6782.
19. S. Szafert and J. A. Gladysz, *Chem. Rev.* 2003, **103**, 4175-4206.
20. I. Eryazici, C. N. Moorefield and G. R. Newkome, *Chem. Rev.* 2008, **108**, 1834-1895.
21. F. Barigelletti and L. Flamigni, *Chem. Soc. Rev.* 2000, **29**, 1-12.
22. V. Balzani, A. Juris, M. Venturi, S. Campagna and S. Serroni, *Chem. Rev.* 1996, **96**, 759-834.
23. V. Balzani and A. Juris, *Coord. Chem. Rev.* 2001, **211**, 97-115.
24. T. Moriuchi, J. Shiori and T. Hirao, *Tetrahedron Lett.* 2007, **48**, 5970-5972.
25. S. P. Cummings, A. R. Geanes, P. E. Fanwick, A. Kharlamova and T. Ren, *J. Organomet. Chem.* 2011, **696**, 3955-3960.
26. Y.-W. Zhong, S.-H. Wu, S. E. Burkhardt, C.-J. Yao and H. C. D. Abruna, *Inorg. Chem.* 2011, **50**, 517-524.
27. M. Velayudham, S. Singaravadivel, S. Rajagopal and P. Ramamurthy, *J. Organomet. Chem.* 2009, **694**, 4076-4083.
28. A. Klein, O. Lavastre and J. Fiedler, *Organometallics*, 2006, **25**, 635-643.
29. C. l. Olivier, B. Kim, D. Touchard and S. p. Rigaut, *Organometallics*, 2008, **27**, 509-518.
30. M. C. B. Colbert, J. Lewis, N. J. Long, P. R. Raithby, M. Younus, A. J. P. White, D. J. Williams, N. N. Payne, L. Yellowlees, D. Beljonne, N. Chawdhury and R. H. Friend, *Organometallics*, 1998, **17**, 3034-3043.
31. S. I. Ghazala, F. D. R. Paul, L. Toupet, T. Roisnel, P. Hapiot and C. Lapinte, *J. Am. Chem. Soc.* 2006, **128**, 2463-2476.
32. L. Medei, L. Orian, O. V. Semeikin, M. G. Peterleitner, N. A. Ustynyuk, S. Santi, C. Durante, A. Ricci and C. Lo Sterzo, *Eur. J. Inorg. Chem.* 2006, 2582-2597.
33. D. Saha, S. Das, S. Mardanya and S. Baitalik, *Dalton Trans.* 2012, **41**, 8886-8898.

34. D. Saha, S. Das, D. Maity, S. Dutta and S. Baitalik, *Inorg. Chem.* 2011, **50**, 46-61.
35. C. Bhaumik, D. Saha, S. Das and S. Baitalik, *Inorg. Chem.* 2011, **50**, 12586-12600.
36. C. Bhaumik, S. Das, D. Saha, S. Dutta and S. Baitalik, *Inorg. Chem.*, 2010, **49**, 5049-5062.
37. D. Saha, S. Das, C. Bhaumik, S. Dutta and S. Baitalik, *Inorg. Chem* 2010, **49**, 2334-2348.
38. S. Das, D. Saha, C. Bhaumik, S. Dutta and S. Baitalik, *Dalton Trans.* 2010, **39**, 4162-4169.
39. J.-L. Xia, X. Wu, Y. Lu, G. Chen, S. Jin, G.-a. Yu and S. H. Liu, *Organometallics*, 2009, **28**, 2701-2706.
40. L. Mercs, A. Neels, H. Stoeckli-Evans and M. Albrecht, *Inorg. Chem* 2011, **50**, 8188-8196.
41. K. Livanov, V. Madhu, E. Balaraman, L. J. W. Shimon, Y. Diskin-Posner and R. Neumann, *Inorg. Chem.* 2011, **50**, 11273-11275.
42. L. F. Joulie, E. Schatz, M. D. Ward, F. Weber and L. J. Yellowlees, *J. Chem. Soc., Dalton Trans.*, 1994, 799-804.
43. R. G. Pearson, *Coord. Chem. Rev.*, 1990, **100**, 403-425.
44. P. Braunstein and F. Naud, *Angew. Chem., Int. Ed.*, 2001, **40**, 680-699.
45. E. D. Cross, U. A. Shehzad, S. M. Lloy, A. R. C. Brown, T. D. Mercer, D. R. Foster, B. L. McLellan, A. R. Murray, M. A. English and M. Bierenstiel, *Synthesis*, 2011, 303-315.
46. J. A. Acosta-Ramirez, M. C. Larade, S. M. Lloy, E. D. Cross, B. M. McLellan, J. M. Martell, R. McDonald and M. Bierenstiel, *J. Mol. Struct.*, 2013, **1034**, 29-37.
47. J. P. Klinman, *J. Biol. Chem.*, 2006, **281**, 3013-3016.
48. N. R. McIntyre, E. W. Lowe, J. L. Belof, M. Ivkovic, J. Shafer, B. Space and D. J. Merkler, *J. Am. Chem. Soc.*, 2010, **132**, 16393-16402.
49. D. P. Halbach and C. G. Hamaker, *J. Organomet. Chem.*, 2006, **691**, 3349-3361.
50. C. G. Hamaker and D. P. Halbach, *Inorg. Chim. Acta.*, 2006, **359**, 846-852.
51. C. G. Hamaker and D. P. Halbach, *Polyhedron*, 2009, **28**, 2228-2232.
52. C. G. Hamaker, O. S. Maryashina, D. K. Daley and A. L. Wadler, *J. Chem. Crystallogr.*, 2010, **40**, 34-39.
53. R. Drozdzak, B. Allaert, N. Ledoux, I. Dragutan, V. Dragutan and F. Verpoort, *Adv. Synth. Catal.*, 2005, **347**, 1721-1743.
54. A. M. Masdeu-Bulto, M. Dieguez, E. Martin and M. Gomez, *Coord. Chem. Rev.*, 2003, **242**, 159-201.

55. D. V. Aleksanyan, V. A. Kozlov, Y. V. Nelyubina, K. A. Lyssenko, L. N. Puntus, E. I. Gutsul, N. E. Shepel, A. A. Vasil'ev, P. V. Petrovskii and I. L. Odinets, *Dalton Trans.*, 2011, **40**, 1535-1546.

56. C. A. Kruithof, H. P. Dijkstra, M. Lutz, A. L. Spek, R. J. M. K. Gebbink and G. van Koten, *Organometallics*, 2008, **27**, 4928-4937.

57. M. Gagliardo, N. Selander, N. C. Mehendale, G. van Koten, R. J. M. Klein Gebbink and K. J. Szabó, *Chem. Eur. J.*, 2008, **14**, 4800-4809.

58. R. Cervantes, J. Tiburcio and H. Torrens, *Inorg. Chim. Acta*, **376**, 525-530.

59. E. D. Cross, A. Acosta-Ramirez and M. Bierenstiel, unpublished results.

- Table of Contents entry:

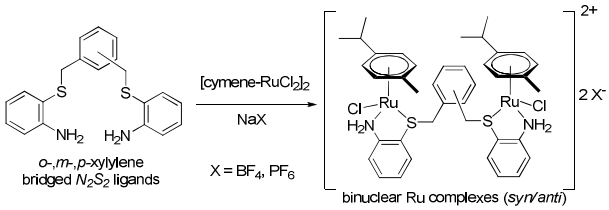

- Summary sentence: "Xylylene bridged N_2S_2-ligands are an excellent ligand platform for binuclear *p*-cymene ruthenium complexes with tunable Ru-Ru distances."